NTNU
Norwegian University of
Science and Technology

TDT4900 Computer Science, Master thesis

FANCY TITLE

Magnus Halvorsen

Spring 2015

Department of Computer and Information Science
Norwegian University of Science and Technology

Supervisor 1: Donn Alexander Morrison
Supervisor 2: Yaman Umuroglu

Assignment

Candidate name: Magnus Halvorsen

Assignment title: Energy efficient machine learning algorithms in hardware

Supervisors: Donn Alexander Morrison and Yaman Umuroglu

Assignment text:

This project will explore the design and implementation of convolutional neural networks (CNNs) in hardware with the intention of improving energy efficiency over traditional implementation in software on a general-purpose CPU. The overall goal is to build a standalone system that (time permitting) could be trained interactively by a user (e.g., to recognise handwriting or faces from a webcam video stream) and then demonstrate learned patterns through recognition of unseen samples.

The energy efficiency of the hardware implementation should be evaluated against software equivalent running on a general-purpose CPU and this evaluation should constitute a major aspect of the report.

The suggested platform is the Zynq FPGA board, but the student can also investigate and weigh the advantages and disadvantages other platforms such as SHMAC.

Abstract

TODO ABSTRACT

Contents

List of Figures

List of Tables

Chapter 1

Introduction

1.1 Motivation

A *Convolutional Neural Network* (CNN) is a deep-learning algorithm which have become an increasingly popular in the last decade. It is considered a state of art technique for object recognition in images and sound, and is applied in application such as video surveillance, mobile robot vision, image search in data centers, and more [1] [2] [3] [4]. With the Internet-of-Things and today's tremendous amount of devices able to capture pictures and videos, the potential for CNNs have vastly increased. By making our devices able to recognize its surroundings there could be a numerous amount of potential interesting applications.

Albeit CNNs perform great in terms of accuracy (see Chapter 3, they are very computational heavy, which have limited their usability until recent years. The computational structure of neural networks is highly parallelizable, which, when exploited, can greatly increase performance. It is for this reason that *general-purpose central processing units* (GPCPUs) performs poorly when computing such networks, as they are primarily designed for effective serial computations, and are thus unable to exploit parallel structure. *Field-programmable gate arrays* (FPGAs), *graphic processor units* (GPUs) and *application-specific integrated circuits* (ASICs) are hardware components that are (or can be) built to heavily exploit parallelism, and have been shown to greatly outperform CPUs in parallel applications [5].

While GPUs performs incredibly well on parallel applications, they have a major drawback: power consumption. With power being the primary cost of data centers and mobile devices operating on a limited power budget [6], GPUs can be unsuitable for several applications. Thus for CNN applications that require lower power and high performance FPGA and ASIC accelerators have become

increasingly popular (see Section 3.2). Simplistically, an ASIC is an processor that is made specifically for one application, while a FPGA is a component that contains a set of programmable logic blocks that can be configured to have the same behaviour as any arbitrary circuit. I.e. a FPGA is a reconfigurable ASIC.

In our previous work, [7], we investigated the mathematical model behind neural networks and purposed a unimplemented accelerator architecture. In this project we have implemented a tweaked version of this architecture on a Zynq FPGA, and constructed all the supporting hardware and software components needed to get it running. In order to test its capabilities we have used it to compute the LeNet-5 [8], which recognizes handwritten digits, and compared its performance to an ARM and laptop CPU.

1.2   Assignment Interpretation

Based on the assignment description text, the following main tasks were identified:

Task 1 *(mandatory)* Implement a hardware accelerator for a Convolutional Neural Network, with the intention of improving energy efficiency.

Task 2 *(mandatory)* Compare to an equivalent software implementation on a general-purpose CPU, primarily in terms of power consumption.

Task 3 *(optional)* Implement said system on a Zynq FPGA board, but weigh the advantages and disadvantages of other platforms such as SHMAC or other FPGA platforms.

Task 4 *(optional)* Extend the system to be able to recognize objects from a web-cam stream.

1.3   Report structure

For the convenience of the reader, we will here provide a quick overview of the topic of the report's chapters.

Chapter 2: Background gives an introduction to the mathematical model of Artificial Neural Networks and Convolutional Neural Networks.

Chapter 3: Related Work gives an overview of the state of the art CNNs, and the most relevant recent hardware implementations.

Chapter 4: Architecture presents our implemented design for a CNN hardware accelerator.

Chapter 5: Results and Discussion compares our design with a equivalent implementation on a ARM and laptop CPU, in terms of performance and energy efficiency, and the hardware resource usage of our design. The chapter will also provide our analysis of the results.

Chapter 6: Future Work presents how our design can be further improved.

Chapter 7: Conclusion provides concluding remarks and a summary of which tasks we were able to complete.

Chapter 2

Background

In order to be able to accelerate a system it is important to understand the mathematical model behind it. For this reason we have included Section 2.1 and 2.2 from our previous work [7], which purposed a theoretical accelerator architecture. The sections will introduce the fundamental mathematics and concepts behind the *Convolutional Neural Network* (CNN) model. They give a basic introduction to both general neural networks and *CNNs*.

2.1 Artificial Neural Networks

An *Artificial Neural Network* (ANN) [9][10] is a computational model that is used for machine learning and pattern recognition. The name and basic concept is inspired by how the animal brain uses a network of neurons to recognize and classify objects. Depending on the input different neurons *activate* (or *fire*), making the brain able to decide what kind of pattern it is detecting.

An ANN can intuitively be viewed as a probabilistic classifier. Depending on the input data it will calculate the probability that the data belongs to a certain *class* (e.g. an object in an image or an investment decision). The network can be trained to recognize different classes by being provided a set of labeled training data, e.g. a set of faces and a set of non-faces. It can then learn to decide whether an image contains a face or not. This is called supervised learning. The network can also be trained unsupervised, by providing it with a set of unlabeled images. The latter technique is used to find hidden structures in the data, by learning the network to recreate the input. But for this project only supervised learning is relevant.

2.1.1 Definition

An ANN consists of a number of layers containing a set of so-called *neurons* (see Figure 2.1), also known as *units*. A neuron takes in a set of values as input (e.g. image pixels), where each value is associated with a respective weight. The input and the weights are multiplied and summed, and the result is used to calculate a non-linear *activation function*. Formally a neurons input and output is defined as:

$$Input : \{x_1, x_2, \ldots, x_n\} = \mathbf{x} \tag{2.1}$$

$$Output : f(\mathbf{w^T x}) = f(\sum_{i=1}^{n} w_i x_i + b) = o \tag{2.2}$$

Where $\mathbf{w}$ is the vector containing connection weights and b is the neuron bias. *f(...)* is the activation function, which eumulates the activation of a neuron in the brain, i.e. it decides whether the neuron is on or off. It also causes the values in the network to have a reasonable value interval. *f(...)* tends to be either:

$$Sigmoid : f(z) = \frac{1}{1 + e^{-z}} \tag{2.3}$$

$$\text{Hyperbolic tagent:} f(z) = tanh(z) = \frac{e^z - e^{-z}}{e^z + e^{-z}} \tag{2.4}$$

The reason these functions are used is that they have the non-linear property, which increases the expressivness of the network. Thus reducing the number of neurons the network needs to solve a given problem. In addition both function have ranges [0, 1] and [-1, 1], respectively, which translates well into probability computation. I.e. you can view the value of the activation function as the probability of that neuron activating.

An ANN consist of n_l layers, each containing a set of neurons. The first layer is *the input layer*, and the last layer is *the output layer*. The layers in between are called *the hidden layers*. Each layer uses the previous layer's output as input. The input layer is provided with the initial input and uses it to calculate the activation function for each of its neurons. The result is propagated to the first hidden layer, and continues up until it reaches the output layer, which provides the final output. This is known as a *feedforward neural network*.

The network takes in two parameters:

$$(\mathbf{W}, \mathbf{b}) = (\mathbf{W}^{(1)}, b^{(1)}, \mathbf{W}^{(2)}, b^{(2)}, \ldots, \mathbf{W}^{(n_l)}, b^{(n_l)}) \tag{2.5}$$
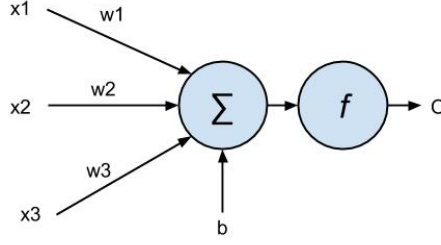
Figure 2.1: A single neuron with three inputs.

Where $\mathbf{W}$ is a 3-dimensional matrix containing the weight matrix for each layer. $\mathbf{W}^{(l)}$ contains the weight matrix for the weights going from layer l to $l+1$. E.g., in the case of Figure 2.2, $\mathbf{W}^{(1)} \in \Re^{3 \times 4}$ and $\mathbf{W}^{(2)} \in \Re^{4 \times 2}$.
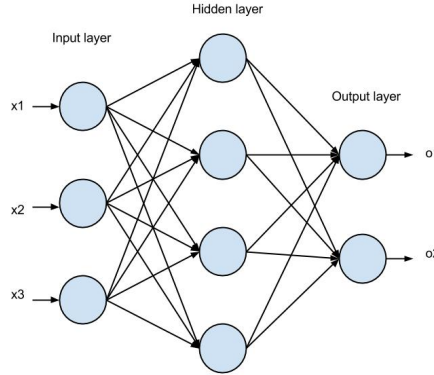
Figure 2.2: An Artificial Neural Network.

2.1.2 Training

During the training of the network it is the parameters $(\mathbf{W}, \mathbf{b})$ that are altered in order to adapt the network to the training data. This is done by providing the network with a set of training samples, where we provide an input and an expected output. By using a cost function we can then figure out how we should tune our weights and biases in order to reduce the error rate. In other words, our goal is to minimize a cost function over a set of training samples. This can be done by using *gradient descent* and the *backpropagation algorithm* [11][12][8].

Let the cost function for a single training example (x, y) be defined as:

$$Cost(\mathbf{W}, \mathbf{b}; x, y) = \frac{1}{2}(h_{\mathbf{W}, \mathbf{b}}(x) - y)^2 \qquad (2.6)$$

Where x is the input, $h_{\mathbf{w}, b}(x)$ is the actual output of our network and y is the correct output. Then the cost function for m training examples $((x^1, y^1), (x^2, y^2), \ldots, (x^m, y^m))$ is:

$$Cost(\mathbf{W}, \mathbf{b}) = \frac{1}{m}\sum_{i=1}^{m} Cost(\mathbf{W}, \mathbf{b}; x^{(i)}, y^{(i)}) + \frac{\lambda}{2}\sum_{l=1}^{n_l-1}\sum_{i=1}^{s_l}\sum_{j=1}^{s_l+1}(\mathbf{w}_{ji}^l)^2 \qquad (2.7)$$

Where the first term is simply the average sum-of-squares error. The second term is the *regularization term*, or *weight decay term*, which tends to reduce *overfitting*. ANNs have a vast number of parameters, i.e. weights, which makes it susceptible to random noise. This can greatly reduce the networks ability to provide correct predictions, but this can be mended by the regularization term.

Based on this we can use gradient descent to compute how we should alter the weights in order to reduce the cost function. One iteration of gradient descent updates $\mathbf{w}$ and b as follows:

$$w_{ij}^{(l)} = w_{ij}^{(l)} - \alpha \frac{\partial}{\partial w_{ij}^{(l)}} Cost(\mathbf{W}, \mathbf{b}) \qquad (2.8)$$

$$b^{(l)} = b^{(l)} - \alpha \frac{\partial}{\partial b_i^{(l)}} Cost(\mathbf{W}, \mathbf{b}) \qquad (2.9)$$

Where α is the learning rate, which is a predetermined constant. w_{ij}^l denotes the weight between neuron j in layer l, and neuron i in layer l+1. b_i^l denotes the bias associated with neuron i in layer l+1.

Note that this would only make us able to compute the gradient for the output layer. In order to perform gradient descent on the hidden layers, we need to propagate the error from the output layer backwards, to the hidden layers. For this we use the *backpropagation algorithm*. Let $o_i^{(l)}$ denote the output of the ith neuron in layer l, and $z_k^{(l)}$ is the weighted sum of the inputs plus the bias for the kth neuron in layer l. Then the *backpropagation algorithm* can be formalized as follows:

1. Perform a feedforward pass, computing the output of every layer.

2. For each output neuron k in the output layer, compute *the error term*:

$$\delta_k = \frac{\partial}{\partial z_k^{(n_l)}} Cost(\mathbf{W}, \mathbf{b}; x, y) = -o_k^{n_l}(1 - o_k^{n_l})(y_k - o_k^{n_l}) \qquad (2.10)$$

3. For each hidden layer $l = n_l - 1, n_l - 2, \ldots, 2$ compute:

$$\delta_i^l = o_i^l (1 - o_i^l) \sum_{j=1}^{s_{l+1}} w_{ij}^l \delta_j^{l+1} \tag{2.11}$$

4. Compute the partial derivative for each weight and bias:

$$\frac{\partial}{\partial w_{ij}^{(l)}} Cost(\mathbf{W}, \mathbf{b}; x, y) = o_j^{(l)} \delta_i^{(l+1)} \tag{2.12}$$

$$\frac{\partial}{\partial b^{(l)}} Cost(\mathbf{W}, \mathbf{b}; x, y) = \delta_i^{(l+1)} \tag{2.13}$$

Now, combining *gradient descent* and the *backpropagation algorithm* we can describe an algorithm to train our network:

1. Initialize the weights $\mathbf{w}^{(l)}$ and b^l to random values for every layer l.

2. Do steps 3 to 5 until the $Cost(\mathbf{W}, \mathbf{b})$ function is low enough or converges. This is referred to as an *epoch*.

3. Set $\Delta \mathbf{w}^{(l)} := 0$ and $\Delta b^{(l)} := 0$ for all l.

4. For i = 1 to m,

    (a) Use the backpropagation algorithm to compute $\nabla_{\mathbf{w}^{(l)}} Cost(\mathbf{W}, \mathbf{b}; x^{(i)}, y^{(i)})$ and $\nabla_b^{(l)} Cost(\mathbf{W}, \mathbf{b}; x^{(i)}, y^{(i)})$ for every layer l.

    (b) Set $\Delta \mathbf{w}^{(l)} := \Delta \mathbf{w}^{(l)} + \nabla_{\mathbf{w}^{(l)}} Cost(\mathbf{W}, \mathbf{b}; x^{(i)}, y^{(i)})$.

    (c) Set $\Delta b^{(l)} := \Delta b^{(l)} + \nabla_{b^{(l)}} Cost(\mathbf{W}, \mathbf{b}; x^{(i)}, y^{(i)})$.

5. Update the parameters:

$$\mathbf{w}^{(l)} = \mathbf{w}^{(l)} - \alpha[(\frac{1}{m} \Delta \mathbf{w}^{(l)}) + \lambda \mathbf{w}^{(l)}]$$

$$b^{(l)} = b^{(l)} - \alpha[\frac{1}{m} \Delta b^{(l)}]$$

2.1.3 Issues with object recognition

While the ANN model have proven useful in several applications, it falls short when it comes to object recognition in images. According to [8] there are three major reasons for this: .

1. **Topology**. A fully connected ANN does not take into consideration the topology of the input. An image has a strong 2D spatial locality correlation, which makes it possible to combine low-order features (edges, end-points etc.) in the same area into higher-order features.

2. **Scalability**. Even small images contains a large amount of pixels/inputs, e.g. a 32×32 image contains 1024 pixels/inputs. A fully connected network with 100 hidden units would then end up with 1024×100 weights that needs to be calculated in the first layer. Thus making it harder to scale for larger images and rather inefficient .

3. **Object variance.** While objects are similar enough, on a higher level, to be grouped together into a class, they can still be very different on a lower level. E.g. a human face have several features that are needed for it to be defined as a face, e.g. eyes, mouth, nose etc. But the size and shape of these features tend to be very different from person to person. While it is possible for a standard ANN to compensate for these internal differences within a class, it would have to make three costly compensations. 1) The network would have to be very large, 2) it would probably contain several neurons with similar weight vectors positioned at different places in the network, and 3) it would require a massive amount of training samples.

2.2 Convolutional Neural Network

A *Convolutional Neural Network* [8] (CNN) is an extension of the *Artificial Neural Network* model, which is made specifically for object recognition in images or speech recognition. It was made in order to solve the issues that the classic ANN model faced.

2.2.1 Definition

The CNN model adds two additional types of layers, in addition to the standard ANN layers: a *convolution layer* and a *subsampling/pooling layer*. The idea behind the two new layers is to exploit the local 2D structure of images, i.e. pixels close to each other are highly correlated. By using local correlation one can extract and combine small local features (e.g. edges, corners, points) into
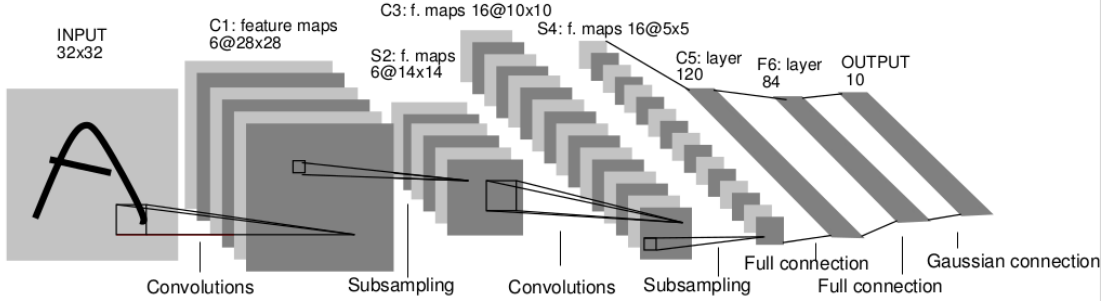
Figure 2.3: An example CNN, the LeNet-5 [8]. It consists of two convolution and subsampling/pooling layer pairs, which are connected to a fully connected ANN with 10 output classes.

higher-order features (e.g. a nose, a mouth, a forehead), which can in the end be recognized as an object (e.g. a face). A full network is illustrated in Figure 2.3.

Convolution layer

The convolution layer extracts a set of features from a set of input images. For each feature, the respective feature is extracted from all the input images and put in a feature map. E.g. if the filter extracts vertical edges, only the vertical edges from all the input images would remain in the resulting feature map. Thus different features can be extracted by having several feature maps that extracts different features.

The extraction is done by performing a *convolution operation* on the image, using a *kernel* that acts like a filter. The kernel is a 2D matrix that contains a set of weights. Depending on values of the weights, convoluting the image with the kernel will have wide range of effects, e.g. sharpening, bluring, edge detection and feature extraction. By training our network we can configure the weights to extract the features we need in order to recognize our desired classes.

After the convolution operation has been performed, a bias is added to every element in the feature map and the result is sent through a non-linear function, e.g. the hyperbolic tangent.

Formally we can define the convolution layer as follows. The layer accepts n images $X_1, X_2, \ldots, X_n$ as inputs, and produces m feature maps, $F_1, F_2, \ldots, F_m$. These feature maps are produced using a set of m learned kernels $W_1, W_2, \ldots, W_m$. Each feature map F_t is then produced by computing:

$$\mathbf{F}_t = Tanh(b_t + \sum_{i=1}^{n} \mathbf{X}_i * \mathbf{W_t}) \tag{2.14}$$

Where $\mathbf{F}$ is the resulting feature map, X is the input image, $\mathbf{W}$ is the kernel matrix, and b is the bias. $X * W$ is the convolution operation, which is defined as:

$$y_{ij} = \sum_{q=1}^{k} \sum_{p=1}^{k} x_{i+q,j+p} w_{qp} \tag{2.15}$$

Where x_{ij} is a value of the input matrix, w_{mn} is a value in the $k \times k$ kernel matrix, and y_{ij} is a value of the output matrix.

E.g. consider the LeNet-5 in Figure 2.3, in the first layer C1 the input is a single 32×32 image which is convoluted with 6 kernels, producing 6 feature maps. Thus $n = 1$ and $m = 6$. The resulting feature maps are then further processed by a subsampling/pooling layer S2 (see next section), which are used as input to the next convolutional layer C3. The six processed feature maps are then convoluted with 16 kernels, producing 16 new feature maps. Thus in this layer $n = 6$ and $m = 16$.

This helps solve the first two issues from Section 2.1.3. The neurons in a feature map share the same kernel, thus the same weights, which greatly reduces the size of the network. The convolution operation applies a 2D filter on the image, which makes the network able to exploit the spatial correlation in the image.

Subsampling/pooling layer
Once a feature has been detected, the exact position become less important. For example, the distance between the mouth and the eyes tend to vary between persons. So in order to make the CNN not too sensitive to the relative placement of features, the accuracy of the all feature maps needs to be reduced. This can be done by subsampling (i.e. partitioning) the feature map into $s \times s$ non-overlapping submatrices, and then perform a pooling operation on each respective matrix. There are two types of pooling operations which are used for CNNs:

- *Max-pooling* extracts the maximum value of the submatrix.

- *Average-pooling* extracts the average value of all the elements in the submatrix.

Given an output of m feature map inputs, each output matrix can be defined as:
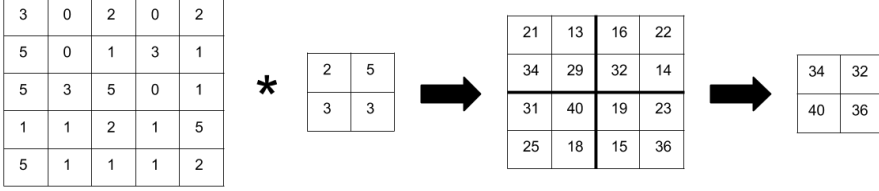
Figure 2.4: Illustration of the convolution and subsampling/max-pooling operations. The leftmost matrix is convulted with a 2×2 kernel, and the resulting matrix is subsampled into four non-overlapping areas where the max value is extracted.

$$\mathbf{O_t} = Tanh(b_t + subsample\_pool(\mathbf{F_t})) \qquad (2.16)$$

Where O_t is the t'th output matrix, b_t is t'th bias, and F_t is the t'th input feature map, and the *subsample_pool()* function's operation is defined as either:

$$o_{ij} = max(x_{i \times s + p, j \times s + q}) \qquad q, p \in 1, 2, \ldots, s \qquad (2.17)$$

or

$$o_{ij} = \frac{1}{c} \sum_{p=1}^{s} \sum_{q=1}^{s} x_{i+p, j+q} \qquad (2.18)$$

Where o_{ij} is a value in the output matrix and f_{ij} is a value in the feature map, c is a trained constant, and s is the dimension of the subsampling size. A max-pooling operation is illustrated in Figure 2.4.

Thus, the subsample/pooling layer helps solve the two last issues from Section 2.1.3. By reducing the accuracy, the network is less sensitive to the difference between instances of a class. This also causes the network size to be smaller, since it does not require neurons to recognize the differences.

Figure 2.4 illustrates the convolution operation and the subsample/max-pooling operation, while Figure 2.5 illustrates the full operation of the convolution and subsampling/pooling layers.

2.2.2 Training

As mentioned, a CNN consists of three types of layers: a convolution layer, a subsampling/pooling layer and fully connected layer. The latter is trained as described in Section 2.1.2, using backpropagation and gradient descent. The two
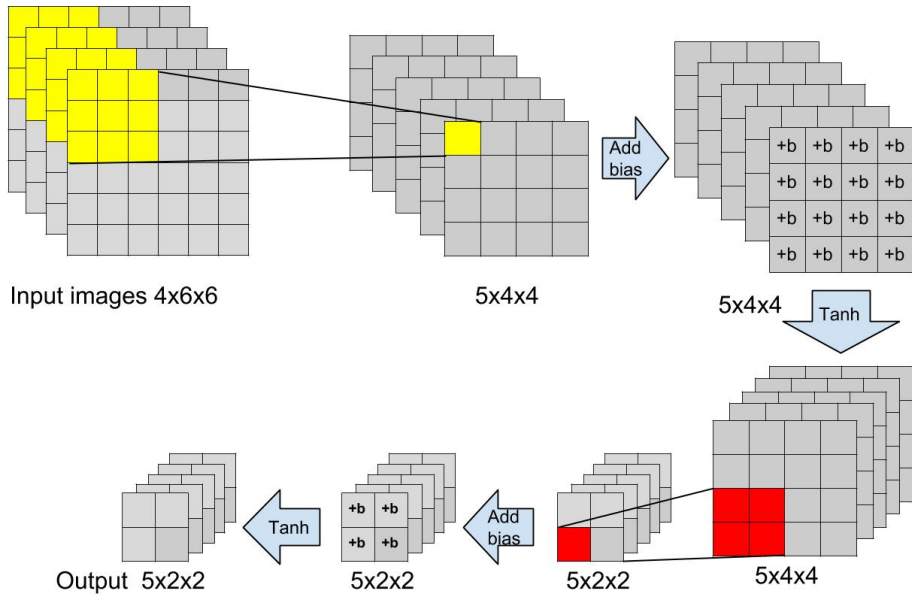
Figure 2.5: A visual overview of the operations performed by the convolution layer and subsampling/pooling layer with four input images. Yellow represents the convolution operation, and red represents the subsampling/max-pooling operation.

other layers use the same general algorithm, but the error δ^l and the gradient of $Cost(\mathbf{W}, \mathbf{b}; x, y)$ is calculated differently.

Since the backpropagation aglorithm starts at the last layer and work its way backwards, the error is first calculated for the fully connected layers. It is then provided to the subsampling/pooling layer, and finally to the convolution layer. Thus we first need to calculate the error for the subsampling/pooling layer, so we can propagate it to the convolution layer.

The subsampling/pooling layer does not contain any weights, and can therefore not be tuned. Thus it only needs to propagate the error it receives. Depending on which pooling operation is used, there are two respective methods for this. For max pooling, the error is simply propagated to the neuron that was chosen as the maximum value, while the rest are set to zero. For average-pooling we have to distribute the error evenly between all the responsible neurons. We therefore define the function *upsample(...)*, which performs the correct propagation operation depending on the type of pooler.

We can now formally define how to calculate the error and the gradient by

simply replacing the equations in step 3 and 4 in the backpropagation algorithm with the following equations. For simplicity we assume that convolution and subsampling/pooling is done in a single layer l.

$$\delta_k^l = upsample((\mathbf{W}_k^l)^T \delta_k^{l+1}) \bullet f'(\mathbf{Z}_k^l) \tag{2.19}$$

Where $(\mathbf{W}_k^l)^T$ is the weight matrix in layer l, δ_j^{l+1} is the error matrix for layer $l+1$, $\bullet$ is the element-wise product (i.e. Hadamard product), $f'(\mathbf{Z}_k^l)$ is the matrix containing the derivative of the activation function, and k indexes the filter number. I.e. it contains $o_{kij}^l(1 - o_{kij}^l)$ for every neuron at index ij in feature map k in layer l.

Using this we can calculate the gradient:

$$\frac{\partial}{\partial \mathbf{w}_k^{(l)}} Cost(\mathbf{W}, \mathbf{b}; x, y) = \sum_{i=1}^{m} (\mathbf{o}_i^{(l)}) * \delta_k^{(l+1)} \tag{2.20}$$

$$\frac{\partial}{\partial b_k^{(l)}} Cost(\mathbf{W}, \mathbf{b}; x, y) = \sum \delta_k^{(l+1)} \tag{2.21}$$

2.3 Potential for parallelism

A vast amount of the computation required by a CNN can be parallelized. Thus, in order to achieve the processing of the network it is important that these potential parallelizations are identified and exploited. The most obvious being:

1. The convolution of a matrix $n \times n$ using a $k \times k$ kernel consists of $(n - k + 1) \times (n - k + 1)$ convolution operation, which each can be done in parallel. Thus convoluting the whole matrix could potentially take only the time it takes to perform one convolution operation.

2. The subsampling/pooling operation can also be parallelized by pooling all of the individual submatrices at the same time.

3. The computation of each of the individual feature maps and their corresponding subsampling/pooling. Which [13] referred to as *inter-parallelism*.

4. It is also possible to parallelize the computation of the feature maps that take more than one matrix as input. This is the case in the subsequent layers after the first. Which [13] referred to as *intra-parallelism*.

5. The activation of each neuron in the fully connected. One option is to parallelize them by creating a binary tree multiplier, where you have n units compute the product of the input and its respective weight, then you

use $\frac{n}{2}$ units to add two of the results each, and so on until you have a single value. This will reduce the time it takes from n time to log_2n time if they can all be done in parallel.

Chapter 3

Related Work

This section will give an overview of the current state of research on Convolutional Neural Networks.

3.1 Convolutional Neural Networks

The mathematical fundamentals for Convolutional Neural Networks was introduced as early as in the 1980s by Kunihiko Fukushima[14][15], in form of the *neocognitron* model. The model was later improved in 1998 by Yann LeCun, Lon Bottou, Yoshua Bengio, and Patrick Haffner - who introduced the *Convolutional Neural Network* model. In 2003 the model was simplified by Patrice Simard, David Steinkraus, and John C. Platt [16], in an attempt to make it easier to implement. The paper also mentions two of the main issues with CNNs: the size of the training set and the time spent training. In order to achieve high enough accuracy a CNN requires thousands of training samples, which needs to be labeled. Processing all of these samples and fine-tuning the networks takes a great amount of processing power, causing training to take days or weeks. These issues are the ones that caused CNNs not to gain popularity before mid-2000. The rise of the Internet, digital cameras, and Big Data have provided us with vast amounts of images which can be used for training. Improvements in the speed and sophistication of computer hardware have reduced the training time from days/weeks to hours. E.g. [17] purposes a GPU implementations which reduced the epoch (see Section 2.1.2) training time from 35 hours to 35 minutes. This demonstrates that highly parallel hardware vastly increases the effiency of neural networks compared to CPUs.

These recent advancements have renewed the interest in neural networks, and increased the research done on the field. As a result CNNs have become a leading

model within pattern recognition for computer vision. This can be illustrated by the fact that CNNs implementations have won several pattern recognition contests in the period 2009-2012, including IJCNN 2011 Traffic Sign Recognition Competition[18] and the ISBI 2012 Segmentation of Neuronal Structures in Electron Microscopy Stacks challenge[19].

3.2 Convolutional Neural Network in Hardware

There have been several proposed hardware architectures during the last decade, and below we will describe the more recent and relevant architectures. If the reader is interested in even older implementations, one can refer to [20], [21], [22], [23], and [24]. We have divided the presented the architectures into two categories, mobile co-processors and server co-processors. The first is small architectures that are intended to fit into resource constrained environments, i.e. mobile applications, while the second is larger architectures that have virtually no resource constraint. But a common design goal for both categories are power efficiency.

Mobile co-processors
In [2] a CNN was implemented on a Virtex-4 SX35 FPGA from Xilinx. In this implementation all the fundamental operations were accelerated by a special-made ALU, and controlled by a 32 bit soft processor using macro instructions. That is, they created macro instructions for convolution, non-linear function, subsampling/pool and dot product between values at identical locations in multiple 2D planes and a vector. Training was done offline, and a representation of the network was provided to the soft processor. With this implementation they were able to process a 512×384 gray-scale image in $100ms$, i.e. 10 frames per second. The design was intended for use in low power embedded vision systems, e.g. robots, and the whole circuit board used less than 15 W.

Farabet and LeCun later improved the mentioned architecture in [25]. In this design they added multiple parallel vector processing units and allowed individual streams of data to operate within processing blocks. They were able to achieve 30 frames per second using 15 W. In addition they predicted a planned ASIC implementation of the system would increase the processing speed and reduce the power to 1 W.

In [13] they explore how they can exploit the parallel nature of CNNs. They introduce two types of parallelism found in CNNs, *inter-output* and *intra-output*. The first one comes from the observation that each feature map and the corresponding subsampling/pooling computation can be done in parallel. This is easily seen in the first layer. The second one refers to that the convolution of several inputs are combined to produce one feature map (see Figure 2.5), where

the individual convolutions can be done in parallel. This one is present in all of the convolution layers after the first layer. They exploit these observations by purposing a dynamically configurable co-processor on a FPGA, which can switch between computing several different feature maps in parallel and processing several inputs to compute one feature map. By doing this they are able to fully utilize the parallel nature of a CNN and reduce the intermediate storage on the FPGA. Using a Virtex 5 SX240T FPGA with 1024 multiply-accumulate units they were able to outperform a 2.3 GHz quad-core, dual socket Intel Xeon, and a 1.35 GHz C870 GPU by 4x to 8x.

[26] presents an architecture they named the *nn-X*. For the implementation they used a Xilinx ZC706 platform, containing a Kintex-7 FPGA and two ARM Cortex-A9. They made a set of *collections* that contained acceleration units for the convolution and subsampling/pooling operations. Each collection also contained a data router which could route data to the accelerator units, or to other collections in order to share data. The convolution and subsample/pooling layer was procssed on the FPGA using the accelerators, while the fully connected layer was processed by the arm processors. The authors claim that this architecture is the fastest and most power efficient of all the purposed architectures for mobile processors, to date. It is able to perform up to 227 G-ops/s, using 8W.

[27] focuses one the challenges of memory bandwidth related to deep convolutional neural networks. They argue that while accelerators are fast, slow memory makes it difficult to saturate the accelerators with enough data. To combat this they purpose a memory access optimized routing scheme, where they try do reduce the number of times a input map has to be transfered from memory to the accelerator. A crucial point here is that in general the output map is the sum of several convoluted input maps. Thus if a accelerator is only able to compute one output map at a time, the input maps have to be transfered to the accelerator several times. This architecture suggested reduces the amount of such transfers by having a DMA for every two accelerator, and making the DMA transfer the same data to both of its accelerators. The accelerators will either produce an intermediate results or a complete output map, depending on how many iterations it has run. There is a total if eight accelerators, four which used to combine intermediate results into complete output maps, and four to compute intermediate results. Using this memory scheme they were able to decrease the memory access by 2x and increase the hardware utilization by 2x.

Server co-processors
Hardware acceleration of CNNs have also gained popularity within the data center field. The Internet and Big Data have made it viable to have servers that performs image classification, image recognition and natural language processing, using CNNs. Since the main expense of data centers are power usage, using specialized

hardware accelerators that provides good performance at low power have gained increased popularity. Thus recently there have appeared architecture suggestions for much bigger FPGAs than the previously mentioned, since size is mostly a problem for mobile applications.

One of the most prominent architectures is the one suggested in [1]. In this paper they present a detailed analysis of computing throughput and memory bandwidth utilization. Using the roofline model [28] they explored the design space in order to detect possible optimizations, including loop tiling, unrolling and pipelining. Based on these analysis they purpose a architecture for an hardware accelerator. What separates this architecture from the previous ones is mainly that the accelerator computes the whole layer in one go, instead of parts of the layer and combining them later. That is, all the input data of a layer is inputted to the accelerator, it computes, and outputs all of the output feature maps of that layer. Previous implementations have primarily accelerated parts of the layer, or one feature map at a time. This greatly decrease the off-chip traffic, which is said to be the main performance sink for CNN accelerators. Such an architecture requires an extensive amount of hardware resources, which is why they implemented it on a Virtex 7. The reward is a throughput of 61.62 GFLOPS, using 18.6 W.

Microsoft, who have experimented on using accelerators for CNNs in their data centers, recently purposed an architecture which exceeds the previous one. In [4] they present an hardware accelerator that fit into a Stratix V D5 FPGA, and that can be integrated in their severs. Again, the main optimization is preventing off-chip memory, which they achieve by using an on-chip data re-distributor, making them able to compute several layers in a row. While the previous mentioned architecture computed one layer at a time, this architecture computes several, boosting the performance by 3x compared to the previous. Thus the system is still slower than a GPU implementation on a Tesla K40, which is 6x faster, but the accelerator is at least 2x as energy efficient.

Chapter 4

Architecture

In this chapter we will present our suggested architecture for a hardware acceler-
ated forward propagation of a Convolutional Neural Network used for recognizing
handwritten digits. The architecuture will be presented in a top-down approach,
starting with the topology and dataset of the network, followed by an overview of
the software used, and finally, the hardware architecture of the accelerator. The
source files for the VHDL and software code used in this project can for the time
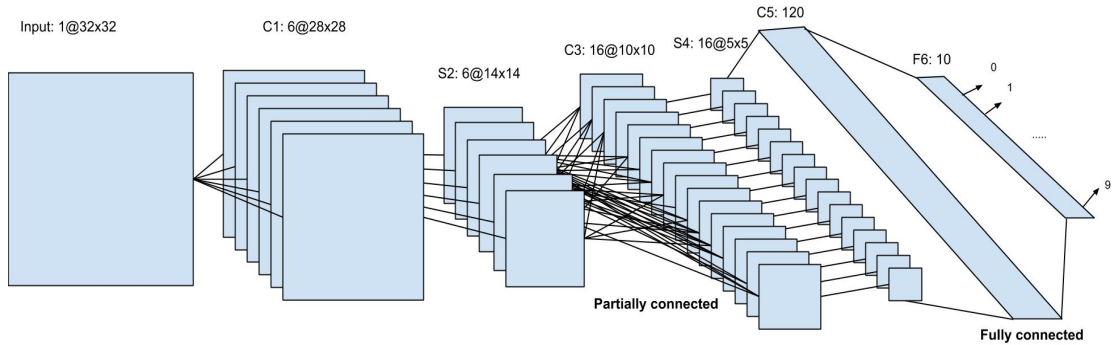being be found at [29]

Figure 4.1: The topology of the implemented network.

4.1 Network Topology and Dataset

We chose to implement a network with a smiliar topology as the LetNet-5 for digit recognition, as seen in Figure 4.1. It consist of six layers:

- **C1, convolution layer**. Takes in a single 32×32 image of an digit. The image is convoluted using six different trained kernels, and outputs six respective 28×28 feature maps.

- **S2, subsampling/average-pooling layer.** Performs the subsample/average-pooling operation on each of the six 28×28 feature maps from the previous layer, using a respective trained value for each map. The resulting output is six 14×14 subsampled feature maps.

- **C3, partially-connected convolution layer.** Takes in six 14×14 feature maps which are partially connected to the sixteen 10×10 output feature maps. These connections are shown in Table 4.2. The connections specifices which inputs are needed to compute a given output. E.g. in order to compute feature map 13, input 2, 4 and 5 are to be convoluted with the 13's kernel. The respective convoluted inputs are then combined into a single matrix, where a bias and activation function is applied to every element - which give the resulting output feature map.

- **S4, subsampling/average-pooling layer.** Performs the subsample/average-pooling operation on each of the sixteen 10×10 feature maps from the previous layer, using a respective trained value for each map. The resulting output is sixteen 5×5 subsampled feature maps.

- **C5, fully connected convolution layer.** Takes in a sixteen 5×5 feature maps which are fully connected to the 120 1×1 output feature maps. Since the size of the output feature maps are a single value, the feature maps are basically standard neurons.

- **F6, output layer**. Takes in 120 neurons which are fully connected to the 10 output neurons. The output neuron with the highest value is the predicted value of the network.

There are three primary reasons for choosing this network. First, it is a relatively small network, which simplifies the implementation by reducing the chances of bugs and memory problems. Secondly, the kernel size of all the convolution layers are the same. This allowed for a less complex implementation, since we did not have to design our accelerator to support different kernel sizes, making it easier for the accelerator support all the convolution layers. Thirdly, this network have been shown to work very well with the MNIST dataset, i.e. our own

	1	2	3	4	5	6	7	8	9	10	11	12	13	14	15	16
1	o				o	o	o			o	o	o			o	o
2	o	o				o	o	o			o	o	o	o		o
3	o	o	o				o	o	o			o		o	o	o
4		o	o	o			o	o	o	o			o		o	o
5			o	o	o			o	o	o	o		o	o		o
6				o	o	o			o	o	o	o		o	o	o

Figure 4.2: Table showing which of the six feature maps from S2 that are needed in order compute the feature maps of C3.

experiments gave an accuracy of 99.1%. Since the aim of this project is exploring hardware acceleration, we did not wish to spend time finding a working topology for a given dataset. Using a topology that has been shown to give high accuracy allowed us to focus more on acceleration rather than topology theory.

As mentioned, we used the *the MNIST dataset*, available at [30]. It consists of 50 000 samples of handwritten digits ranging from 0-9, where 40 000 of the samples are used for training and 10 000 samples are used to determine the accuracy of the network.

4.2 What to accelerate

In order to decide which part of the network that should be accelerated one has to determine the most computational expensive part of the network. In the literature (see Chapter 3 there is a common consensus that the convolution layer is the most demanding layer, and [25] and [1] states explicitly that it amounts to about 90% of the total processing. We have confirmed this number in our own experiments, through a simple mathematical analysis of the network and by profiling a software implementation of the network.

Table 4.1 shows the number of connections for each layer in the network. Each connection corresponds to a multiply-and-accumulate (MAC) operation, e.g. 122304 MAC operations are required to compute C1. Since the number of activation functions to be computed is strongly correlated to the number of connections, we refrained from including them in the analysis. We see that 97% of the computations in our network is performed in the convolution layers, giving a clear indication of what layers should be accelerated.

Layer	Connections	Percentage
$C1$	122304	0.37
$S2$	5880	0.02
$C3$	151600	0.46
$S4$	2000	0.006
$C5$	48120	0.14
$F6$	1200	0.004
$Total$	331104	1.0

Table 4.1: An overview of the number of connections in the network layers.

We also decided to accelerating the subsampling/pooling layers, even though only 0.8% of computations are done there. The reason for this that we were able to make a design where the subsampling/pooling could be done virtually in parallel with the convolution, at a minimal cost to hardware resources (see Section 4.4.6. We deemed the small cost worth the 0.8% potential performance boost. But more importantly, it makes our architecture eaiser to extend to compute several layers in a row, without going back to software, which would greatly reduce off-chip traffic and performance (see Chapter 6).

4.3   Software Architecture

This section gives an overview of software architecture used to compute the network and to control the accelerator.

4.3.1   Network Software

We have made extensive use of Taiga Nomi's C++ framework for neural networks, available at [31], in our project. The framework was used in order to train the parameters of our network, for measuring the efficency of a pure software implementation, and as a basis for the implementation that uses the hardware accelerator. The framework treats each layer in the network as a seperate software module, which makes it easy to swap diffrent implementations of a layer. This simplified the process of integrating the hardware accelerator into the network, since we could simply exchange the original modules with our own.

Figure 4.3 A shows a simplified version of the architecture of the pure software implementation of our network. Each layer contains a set of pretrained weights which are loaded before the network starts processing the images. When an image is inputted to the first layer, it performs the calculations described in Chapter 2 in software, and propegates the result to the next layer.

Figure 4.3 B shows how the original software was changed in order to make use of the accelerator. As mentioned, we decided to accelerate the convolutional layer and the subsample/average-pooling layer, thus we wrote a new software module that would handle both operations. But instead of computing the operations in software, the new module transfer the input data and the weight to the hardware accelerator and extracts the result from the computations.

We decided against accelerating layer C5. The main reason being that in its current form, the accelerator is only able to compute one feature map at a time. Each computation comes with a certain amount of overhead, i.e. transfering data to/from the accelerator and configuring it. Thus for C5, which takes in 120 5×5 matices, we figured that input was so numerous and so small that it would cause too much overhead in order to be efficient. Though this is mostly guesswork, and should be tested before any absolute conclusion is reached. But due to lack of time, this was saved for future work.
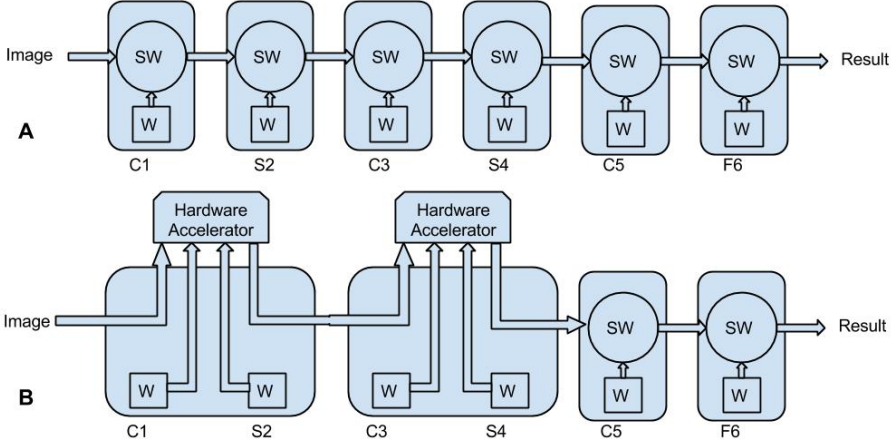

Figure 4.3: A simplified overview of the software architecture with and without hardware acceleration.

4.3.2 Hardware driver

A driver for the accelerator was written in order to create a simple and easy to use interface to the hardware. As mentioned, the accelerator can only compute on feature map at a time, thus the input to the driver is all the data required to compute said feature map. That is, a set of images, their respective kernels and bias, the average pooling constant and its respective bias. The driver then feeds

this data to the accelerator, and returns the computed feature map.

In order to control the accelerator, the driver accesses two memory-mapped control registers. The first registers is used to set which layer is currently going to be processsed, i.e. C1/S2 or C3/S4, and the second one is used to start the accelerator when the input data is ready.

For data transfer the driver uses a *direct memory access controller* (DMA) IP from Xilinx. This is where most of work on the driver had to be done, since the DMA interface is much more complex compared to the accelerator interface. The DMA is configured to transfer the weights and image(s) to the accelerator's input buffer, and extract the data from the output buffer. Since the output buffer is a FIFO, the DMA is able to extract each output value as they are produced, instead of waiting for the accelerator to finish and then transfer all the output data.
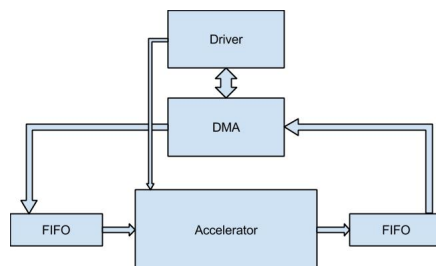

Figure 4.4: The interaction between the driver, DMA and accelerator.

4.4 Hardware Architecture

In this section we will describe the hardware architecture of the system as a whole, and more specifically, our accelerator. Do note that the descriptions and the figures are simplified to some extent. This simplication is done with the intent avoiding complex description and explainations. We will rather focus on conveying the important ideas behind the design, instead of describing every tiny detail of the architecture.

4.4.1 Overview of Hardware Achitecture

4.4.2 Accelerator Interface

The accelerator has three bus interfaces that are used to control it. The first is a slave *Advanced eXtensible Interface* (AXI) interface which is used to write

the two control registers, and reading a set of status registers of the accelerator. The status registers are mostly used for debugging, i.e. reading various crucial values inside the accelerator, but also to determine whether the accelerator is currently processing. The bus is connected to the ARM processor, to allow direct communication between software and hardware.

The second bus interface is a slave *AXI-Streaming* (AXIS) interface, which is used to stream the data input into the accelerator. The interface is connected to a *first-in-first-out* (FIFO) buffer, where all the data required by the accelerator is stored until the accelerator is ready to consume them.

The third bus interface is a master AXIS interface, which is connected to another FIFO buffer. The computed feature map is streamed out of the accelerator into the buffer, and stored there until the DMA moves the data back to software control.

4.4.3 Accelerator Architecture

As previously stated, the accelerator takes n images as input, $I_1, I_2, \ldots, I_n$, n respective kernels $K_1, K_2, \ldots, K_n$, two biases, and outputs a single processed image O. Using the input images, the kernel and the bias, it performs the operations of the convolution and subsampling/pooling layer for a single feature map. Thus the output O is a subsampled/pooled feature map that has been produced by convoluting the images $I_1, I_2, \ldots, I_n$ with the kernels $K_1, \ldots, K_n$.

The accelerator can thus compute the whole convolution and subsample/pooling layer by doing the above computations for all the output feature maps in the layer. One can exploit inter-parallelism by making several instances of the accelerator run in parallel. One can also exploit intra-parallelism, but then one need to connect the different accelerator instances so they can add up the results from the convolutions without using the intermediate convolution buffer, as described in [13]. Unfortunately, within the given timeframe we were unable to get a system working that exploited inter- and intra parallelism. But the architecture is designed to be easily extendable to support this, given more development time.

The accelerators consists of five major components (Figure 4.5):

- **The convoluter**. Performs the convolution operation on the input.

- **The intermediate convolution buffer**. Since the resulting feature map is the sum of the convolutions of all the input images (with the exception of the first layer), this buffer is needed to store the intermediate results from the previous convolution, so that it can be accumulated with the current convolution. In the first layer of the network there is only one input image (i.e. $n = 1$), thus no summation is needed.

- **Tanh**. Performs the non-linear hyperbloc tangent function on the feature maps.

- **Subsample/average-pooler**. Performs the subsample/average-pool operation on the feature map.
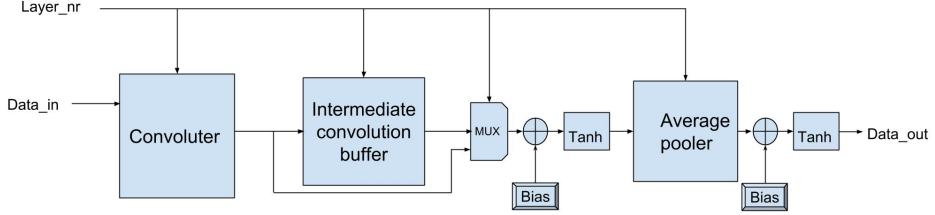

Figure 4.5: The architecture of Imagezor.

The *layer_nr* signal is used to specify whether it is C1/S2 or C3/S4 that is being computed. The input image in the first layer is bigger than the images in the second (32×32 vs 14×14), which the convoluter and the average pooler need to (see Section 4.4.4 and 4.4.6). In addition in the second layer the intermediate convolution buffer needs to be activated so it accumulate and store all the convolutions needed to compute a single feature map. The mux is used to control which data to propagate to the average pooler, directly from the convoluter (C1/S2) or from the buffer (C3/S4).

In order to reduce resources spent and execution time, the accelerator uses Q16.16 fixed-point arithmetic, which is shown to give virtually the same network accuracy as floating-point arithmetic[32] [33] [34]. Something that has been confirmed by our own experiments. In order to implement fixed point arithmetic and fixed to float conversion we used the ieee proposed libaries by David Bishop, available at [35].

In the following sections below we will provide a more detailed description of the convoluter, the hyperbolic tangent unit and the average pooler.

4.4.4 The Convoluter

This module is inspired by [2]. The input is a $n \times n$ image, and the output is a $(n - k + 1) \times (n - k + 1)$ feature map, using a $k \times k$ kernel. The kernel is stored in internal registers that must be rewritten for each different feature map that is to be computed. Every clock cycle the module takes in a pixel as input, and after a certain delay it will output a processed pixel almost every cycle. Each pixel is inputted once, left to right, one row at a time.

It consists of 2D grid of multiply and accumulate (MAC) units which represents the convolution kernel. Thus the grid dimension is equal to the kernel dimension. In every MAC unit there is a register that contains the respective kernel weight. In every clock cycle the MAC units multiply the input pixel with its weight, and then accumulates the result from the previous cycle of the MAC unit to the left.

At the end of each row of MACs there is $n - k$ shift registers. The result of the last MAC in each row is stored in the first shift register, and the first MAC in each row takes the value of the last shift register of the previous row as accumulation input. The exception being the absolute first and last MAC unit. Every clock cycle the values in the shift registers are shifted to the right.
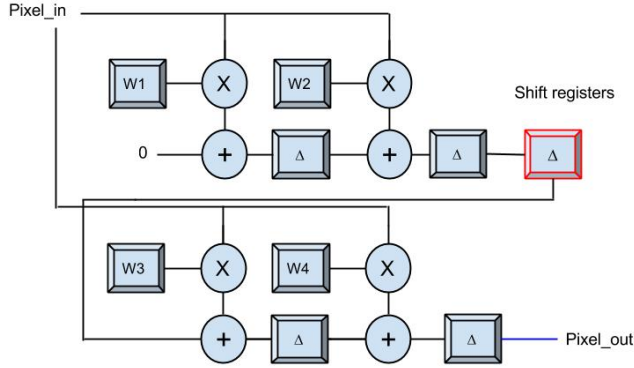

Figure 4.6: The convoluter, when $n = 3$ and $k = 2$.

By providing this delay you only have to input each pixel once during the convolution. Generally every pixel is needed for $k \times k$ convolution operations (the exception being the pixels close to the boarders of the image). Thus the shift registers are used to store the intermediate values of the convolutions until a pixel that is needed for the respective convolution operation is inputted.

The delay these shift registers cause are the reason for the delay before valid output pixels are produced. Thus from when the convolution starts, the output will not be valid before $k - 1$ rows of the image have been processed. And for every new image row, there will be a k cycle delay before the output is valid. The reason for this delay intuitively understood by remembering that the input image is a $n \times n$ matrix, while the output matrix is a $(n - k + 1) \times (n - k + 1)$ matrix.

Since the two layers in the network have different image sizes, but uses the same kernel size, we can use the module for both layers. This is done by having the control signal *layer_nr* decide how many of the shift registers that are to be

Constants
$m_1 = -0.54324$
$m_2 = -0.16957$
$c_1 = 1$
$c_2 = 0.42654$
$d_1 = 0.016$
$d_2 = 0.4519$
$a = 1.52$
$b = 2.57$

Table 4.2: The constant used for the hyperbolic tangent approximation.

Conditions	Output
$0 \leq |x| \leq a$	$sign(x) \times [0.5 \times m_1 \times |x|^2 + c_1 \ times|x| + d_1]$
$a \leq |x| \leq b$	$sign(x) \times [0.5 \times m_2 \times |x|^2 + c_2 \ times|x| + d_2]$
$otherswise$	$signed(x)$

Table 4.3: The piecewise linear approximation of the hyperbolic tangent.

used during convolution. In the first layer all of the shift registers are used, but in the second only a subset is used. I.e. $n - k + 1$ of shift registers are used in each row, where n is either 32 or 14.

The loading of the weights takes $k \times k$ clock cycles, and the processing of the image takes $n \times n$ clock cycles. Thus the total number of cycles it takes to perform a full convolution of an image is $n \times n + k \times k$. But based upon the papers refered to in Section 3 it seems that n tends to be larger than k. E.g. for the first layer in the LeNet-5 [8], $n = 32$ and $k = 5$, the loading of the weights take 25 clock cycles and the image processing 1024 cycles. This means that the execution time of the convoluter is primairly bounded by the size of the image. But the size of the kernel decides the hardware resource cost of the module, since it requires $k \times k$ DSP slices on the FPGA.

4.4.5 The Hyperbolic Tangent

This module is based upon [36] using *piecewise linear approximation*. It takes input a single value x and outputs a linear approximation of the hyperbolic function. Using a lookup table (Table 4.3) and the constants from Table 4.2 the module decides which linear approximation to use. In order to meet the timing constraints on the FPGA the module has a pipeline length of three.
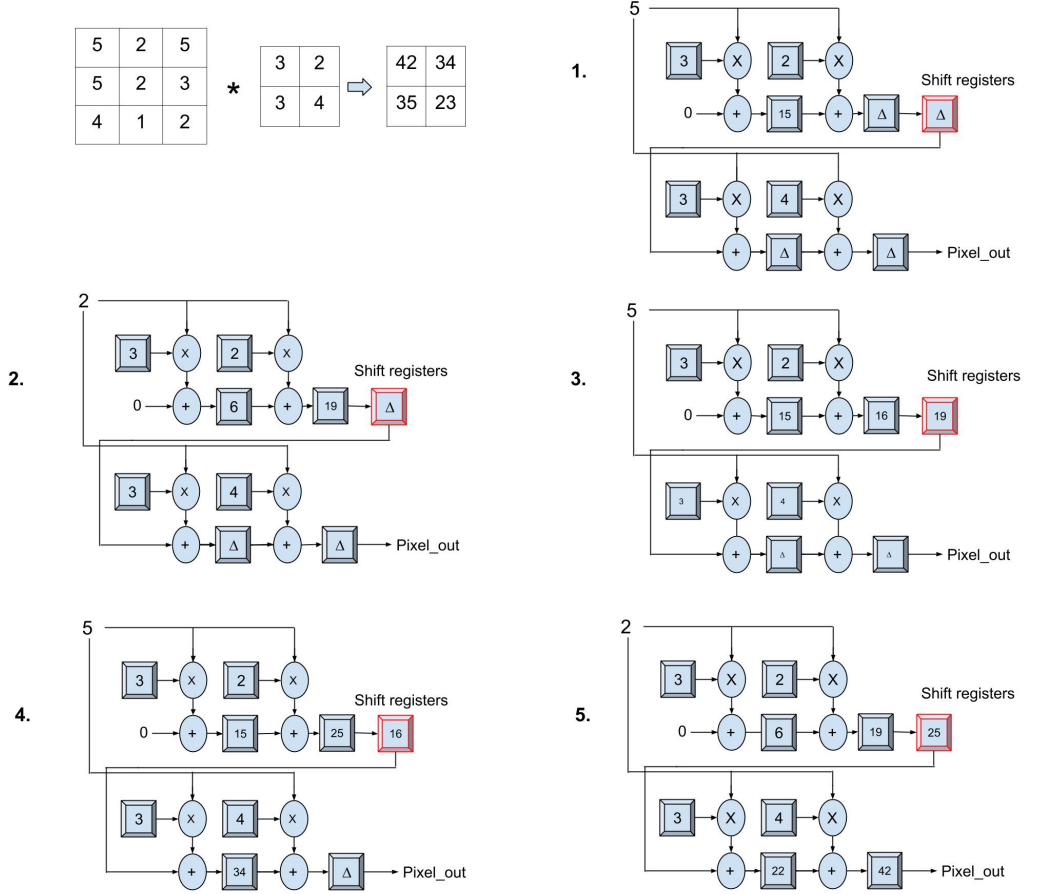
Figure 4.7: Example showing the five first clock cycle of an convolution. The weights of the kernel is already loaded into the MAC units, and every cycle a new pixel from the image in inputted. In the last example you can see that 42 is provided as the first output.

4.4.6 The Average Pooler

The average pooler performs the subsample/average-pooling operation described in Section 2.2.1. The input is a $(n-k+1) \times (n-k+1)$ feature map, and the output is a $(n-k+1)/p \times (n-k+1)/p$ subsampled/average-pooled feature map, where p is the dimension of subsample neighborhood.

The average pooler performs basically two operations, pooling and averaging. The input is divided into $p \times p$ non-overlapping neighbourhoods, which are also refered to as pools. The pooling operation consist of simply summing the data within the respective neighbourhoods. The averaging operation is to multiply the summed pools with a trained average value, which produces a valid output. Figure 4.8 gives an overview of the average pooler architecture, where the SUM module and the shift registers are used for the pooling operation, while the trained C value is used to average the sums.

Since the input is a 2D matrix that is inputted one value at a time left to right, one row at a time, the average pooler will have to keep track of data from $(n - k + 1)/p$ different neighbourhoods simultaniously. That is, after the average pooler has received p inputs from the first neighbourhood, it will next receive p inputs from the next neighbourhood, and so on until the end of the first row is reached. It will then receive data from the first neighbourhood again. This will continue until it has processed p rows, after which it will have processed the first $(n-k+1)/p$ neighbourhoods, i.e. a row of neighbourhoods. It can then continue with the next row of neighbourhoods.

In order to keep track of $(n - k + 1)/p$ neighbourhoods at a time, the average pooler contains a set of $(n - k + 1)/p - 1$ shift registers which are used to store the intermediate sum of the neighbourhoods. The sum module keeps track of the current neighbourhood and accumulate the input data if it belongs to said neghbourhood. When a new neighbourhood is about to be inputted all the shift registers are shifted one to the right, and the sum module extracts the value of the rightmost register.

The control unit keeps track of when to shift the registers and when a neighbourhood is fully summed. To do this the unit contains two counters, *row_num* and *column_num*. When a new pixel is inputted the *column_num* counter is incremented, and when it reaches the end of the row the *row_num* counter is incremented. Every time *column_num mod p = 0* another pool is encounted, and the shift registers are shifted one to the right. When *column_num mod p = 0* and *row_num mod p = 0* the final value in a pool has been reached, and the final sum is multiplied with the trained value C and outputted.

The execution speed of the average pooler module is bounded by the size of the feature map, $(n - k + 1) \times (n - k + 1)$ clock cycles, finishing one cycle after the last pixel has been inputted. Thus by streaming the output of the convoluter to the average pooler, both will finish only a few cycles apart, effectively running both jobs in parallel. The resource usage of the module is bounded by the size of the subsampling dimension, since it requires a number of shift registers equal to the size of the dimension. In addition is consumes one DSP, which is used for the averaging operation at the end. But essentially its resource usage is quite low.
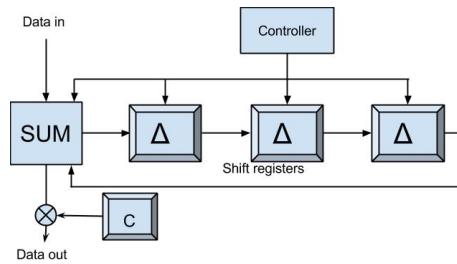
Figure 4.8: The average pooler. The summation module and the shift registers are used to sum up the respective pools. The trained value C is used to average the summed pools.

Chapter 5

Results and Discussion

This chapter will present the results from performance testing our purposed architecture. Section 5.1 will present the setup to our experiments and their respective results, while Section 5.2 will provide our analysis of the results.

5.1   Results

5.1.1   Hardware Resources

The architecture described in Chapter 4 was prototyped on an *Avnet Zedboard*, containing a *Xilinx Zynqq-7020 All Programmable System-On-Chip* (SoC). The SoC contains two ARM Cortex-A9 processors, and a Artix-7 FPGA.

The main reason for choosing this system was that it contains four DMA channels, and 220 DSP slices, which should have allowed us to run four fully saturated accelerators in parallel. Unfortunately resource constraint for our architecture turned out to be *look-up tables* (LUTs)

In this prototype we were only able to use one of the two ARM processors for controlling the accelerator(s) and processing the layers that were not accelerated. Preferably we should have used both for processing layer C5 and F6, but we were unable to do so due to time constraints.

(Not done yet, will add more information on what hardware resources on the FPGA was used, and how this changes when adding more accelerators).

5.1.2   Performance

In order to determine the execution speed and power efficiency of our system we have compared it to the ARM Cortex-A9 CPU on the Zedboard and an ASUS

X550JK laptop with a Intel Core i7 4710HQ CPU. Both CPUs ran the pure software implementation of the CNN, while our system used a combination of hardware and software, as described in 4. We ran our own system with three different configurations:

- Accelerating layer C1 and S2.

- Accelerating layer C1, S2, C3 and S4.

- Accelerating layer C1, S2, C3 and S4. In addition, the input images was preprocessed from 32-bit floating point to Q16:16 fixed point. Thus the input to the accelerator does not have to be converted during execution.

In order to determine the energy efficiency of the different systems we used the metric *images/Watt*, i.e. number of images processed per Watt. Note that these images are 32×32, and thus processing one image corresponds to 331104 multiply-and-accumulate operations. We also included a metric for measuring execution speed, using images/second. Despite power efficiency being the main focus of this assignment, execution speed can be interesting for several applications and is closely related to power usage.

The measurements were done by timing the processing of 10 000 images from the MNIST dataset, while measuring the power consumption.

Total board power was determined by measuring over pin 1 and 2 on J21 on the Zedboard during execution. With the FPGA programmed and the accelerator activated the board measured to 4.68 W, while the ARM processor alone measured to 4.32 W. We were unable to measure the power consumption of the laptop directly, and therefore used the power estimation provided by ASUS, being 120 W [37].

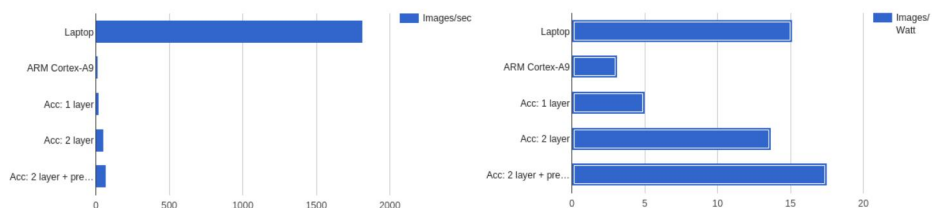The results can be seen in Figure 5.1.

Figure 5.1: The execution speed and power efficiency measured in number of images processed.

We also decided to perform the same measurements when processing only the layers we have hardware accelerated, i.e. C1, S2, C3 and S4. This allowed us to compare the accelerator's performance more directly against the pure software implementations, since layer C5 and F6 shows to be the major bottleneck when processed on the ARM processor. The results are shown in Figure 5.2.
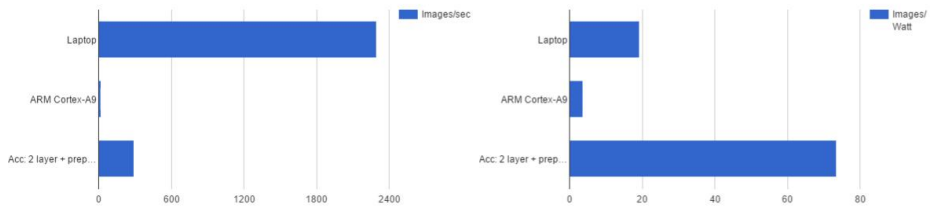

Figure 5.2: The execution speed and power efficiency measured in number of images processed.

5.2 Discussion

5.2.1 Hardware Resources

5.2.2 Performance

As can be seen from the Figure 5.1 the accelerator provides a significant boost to both execution and power performance compared to the ARM processor. Accelerating layer C1 and S2 provides a 1.6x speedup, while accelerating C1, S2, C3 and S4 provides a 4.3x speedup. Which is interesting since both layers computes about the same amount of connections (see Table 4.1), so why is the ARM processor able to compute C1 faster than C3? We deem that the most probable reason is the cache and memory accesses. In layer C1 the input image can be loaded into cache once and stay there for the duration of the processing of the layer. While in layer C3 there is a set of different input maps and kernels that is required to compute a single output map, thus reducing the ARM processors ability to utilize the cache.

Figure 5.2 shows the performance when executing the layers that we have accelerated. Here we clearly see how much the accelerator outshines the ARM processor, with a 21x speedup. This also shows that the current bottleneck is now layer C5 and F6. In Section 4.2 we deemed unlikely to be worth it to accelerate C5, but these results actually make a strong case for it.

Compared to the ASUS X550JK our architecture is currently a lot slower, i.e. 26x slower. This is expected, since the laptop contains a state of the art CPU which is highly optimized for execution performance by Intel, while our accelerator is only a prototype. In addition, this network is a relatively small compared to the ones described in Chapter 3, consequently leading to less parallelism to exploit. In addition when the input maps become to large to fit into cache, it is likely that the laptop's performance will drop. Thus with larger networks we predict that the difference between the execution time will decrease.

But while our accelerator performs worse in terms of execution speed it performs better in regard to power efficiency in some areas. When running all the layers, our system achieves 15.2 images/Watt while the laptop achieves 15.1 images/Watt, i.e. practice the same. But if we look at only the layers accelerated we see that our accelerator is 3x as power efficient. Based on this we believe that our system will outperform the CPU if the features mentioned in Chapter 3 are implemented.

Chapter 6

Future work

Developing a convolutional neural network hardware accelerator is a complex and time consuming task. There are thus several performance related improvements that we would wish to have implemented and tested, but sadly we ran out of time. In this chapter we will give an overview the planned, but unfinished, features we would wish to extend to our current architecture. The features are listed in a priority order, and we will give some indication of how much work is required to implement said features.

1. **Acceleration of layer C5.**

   - Will probably try this before delivering.

2. **Explore ways to reduce the resource usage.**

   The primary focus of this project has been to get the prototype up and running, and little thought have gone to examine ways to minimize resource consumption. Currently we only have enough resources to fit two accelerators on the board. Thus if we wish to extend the design and/or run several accelerators in parallel, we either need to change to a bigger board or minimize the resource usage of our design. Any future work would do well to explore this area.

3. **More accelerators in parallel.**

   Currently we are only running two accelerators in parallel, which both have a respective DMA that moves their input and output data. The maximum DDR bandwidth is at about 3.2 GB/s, and each DMA has access to a *high-performance* port which can deliver up to 800 MB/s. This effectively means that we are exploiting half of the available DDR bandwidth. Given a big

enough hardware platform or improvements to resource usage, as mentioned in the above point, this feature should be simple to implement.

4. **Stay in hardware, instead of going back to software for next layer**

   The main reason [1] and [4] achieved high performance was by reducing off-chip traffic. In the current state of our system, software has to be involved for every feature map to be computed, and data is being transfered back and forth between software and hardware several times. This is inefficient. Thus extending the system with logic that can redistrubute the output maps as new input maps without involving software could provide a substantial performance boost. But it will increase resource usage and development time, and will probably require a bigger board. Both the mentioned papers used FPGAs at the size of a Virtex 7.

5. **Stream data through accelerator, instead of filling the buffer first.**

   Currently all the data required for computations are loaded into a buffer before it is processed by the accelerator. Changing it so that the data can be streamed directly into the accelerator would provide two potential benefits: 1) faster processing, since data can be processed while the DMA is transfering data to the accelerator, 2) reduced storage on chip, since we no longer need to store all the data in an input buffer. Should be fairly easy to extend the design for this, but due to time constraints, and the gains probably not being that great, it was not prioritized.

6. **Hardware accelerate float to fixed.**

   Currently our system pre-processes the image and weights into fixed point before processing them. If this system were to be integrated into system using floating points it would be beneficial to do this transformation in hardware. Currently we are able to do fixed point to floating point in hardware using only one clock cycle, and thus we believe it should be possible to do the same for float to fixed.

7. **Training on hardware.**

Chapter 7

Conclusion

Bibliography

[1] Chen Zhang, Yijin Guan, Peng Li, Bingjun Xiao, Guangyu Sun, and Jason Cong. Optimizing FPGA-based Accelerator Design for Deep Convolutional Neural Networks. *Proceedings of the 2015 ACM/SIGDA International Symposium on Field-Programmable Gate Arrays*, pages 161–170, 2015.

[2] Clément Farabet, Cyril Poulet, Jefferson Y. Han, and Yann LeCun. CNP: An FPGA-based processor for Convolutional Networks. *FPL 09: 19th International Conference on Field Programmable Logic and Applications*, 1(1):32–37, 2009.

[3] Shuiwang Ji, Ming Yang, and Kai Yu. 3D convolutional neural networks for human action recognition. *IEEE transactions on pattern analysis and machine intelligence*, 35(1):221–31, 2013.

[4] Kalin Ovtcharov, Olatunji Ruwase, Joo-young Kim, Jeremy Fowers, Karin Strauss, and Eric S Chung. Accelerating Deep Convolutional Neural Networks Using Specialized Hardware. Technical report, Microsoft Research, 2015.

[5] Eric S. Chung, Peter a. Milder, James C. Hoe, and Ken Mai. Single-chip heterogeneous computing: Does the future include custom logic, FPGAs, and GPGPUs? *Proceedings of the Annual International Symposium on Microarchitecture, MICRO*, pages 225–236, 2010.

[6] M Duranton, K De Bosschere, and J Maebe. The hipeac vision for advanced computing in horizon 2020. 2013.

[7] Magnus Halvorsen. Convolutional Neural Networks and their Potential Hardware Acceleration. Technical report, 2014.

[8] Yann LeCun, Léon Bottou, Yoshua Bengio, and Patrick. Haffner. Gradient-Based Learning Applied to Document Recognition. *Proceedings of the IEEE International Conference on Computer Vision*, 1998.

[9] Marvin Minsky and Seymour Papert. *Perceptrons: an introduction to computational geometry.* 1969.

[10] Christopher M. Bishop. *Pattern Recognition and Machine Learning.* Springer Science+Buisness Media, LLC, 2006.

[11] DE Rumelhart, GE Hinton, and RJ Williams. Learning representations by back-propagating errors. *Nature*, 323:533–536, 1986.

[12] J. Leonard and M. A. Kramer. Improvement of the backpropagation algorithm for training neural networks. *Computers & Chemical Engineering*, 14(3):337–341, 1990.

[13] Srimat Chakradhar, Murugan Sankaradas, Venkata Jakkula, and Srihari Cadambi. A dynamically configurable coprocessor for convolutional neural networks. *Proceedings of the 37th annual international symposium on Computer architecture - ISCA '10*, page 247, 2010.

[14] Kunihiko Fukushima. Neocognitron: A Self-organizing Neural Network Model for a Mechanism of Pattern Recognition Unaffected by Shift in Position. *Biol. Cybernetics*, 202:193–202, 1980.

[15] Kunihiko Fukushima and Sei Miyake. Neocognitron: A new algorithm for pattern recognition tolerant of deformations and shifts in position. January 1982.

[16] PY Simard, Dave Steinkraus, and JC Platt. Best practices for convolutional neural networks applied to visual document analysis. *Seventh International Conference on Document Analysis and Recognition*, 2003.

[17] Dan C Cires, Ueli Meier, Jonathan Masci, and Luca M Gambardella. Flexible , High Performance Convolutional Neural Networks for Image Classification. *IJCAI'11 Proceedings of the Twenty-Second international joint conference on Artificial Intelligence - Volume Volume Two*, pages 1237–1242, 2011.

[18] Dan Cirean, Ueli Meier, Jonathan Masci, and Jürgen Schmidhuber. Multi-column deep neural network for traffic sign classification. *Neural networks : the official journal of the International Neural Network Society*, 32:333–8, August 2012.

[19] D Ciresan, Alessandro Giusti, Luca M. Gambardella, and Jürgen Schmidhuber. Deep neural networks segment neuronal membranes in electron microscopy images. *Advances in Neural Information Processing Systems*, (25), 2012.

[20] R.G. Girones and a.M. Salcedo. Implementation with FPGAs of a pipelined on-line backpropagation. *ICECS'99. Proceedings of ICECS '99. 6th IEEE International Conference on Electronics, Circuits and Systems (Cat. No.99EX357)*, 2:8–11, 1999.

[21] K Benkrid and S Belkacemi. Design and Implementations of a 2D Convolution Core for Video Applications on Fpgas. *Digital and Computational Video, 2002. DCV 2002. Proceedings. Third International Workshopand Computational Video, 2002. DCV 2002. Proceedings. Third International Workshop*, (November):85–92, 2002.

[22] F. Cardells-Tormo and P. Molinet. Area-efficient 2-D shift-variant convolvers for FPGA-based digital image processing. *IEEE Workshop on Signal Processing Systems Design and Implementation, 2005.*, pages 209–213, 2005.

[23] Hui Zhang, Mingxin Xia, and Guangshu Hu. A multiwindow partial buffering scheme for FPGA-based 2-D convolvers. *IEEE Transactions on Circuits and Systems II: Express Briefs*, 54(2):200–204, 2007.

[24] Antony W. Savich, Medhat Moussa, and Shawki Areibi. The impact of arithmetic representation on implementing MLP-BP on FPGAs: A study. *IEEE Transactions on Neural Networks*, 18(1):240–252, 2007.

[25] Clement Farabet, Berin Martini, Polina Akselrod, Selcuk Talay, Yann Le-Cun, and Eugenio Culurciello. Hardware accelerated convolutional neural networks for synthetic vision systems. *Proceedings of 2010 IEEE International Symposium on Circuits and Systems*, pages 257–260, May 2010.

[26] Vinayak Gokhale, Jognhoon Jin, Aysegul Dundar, Berin Martini, and Eugenio Culurciello. A 240 G-ops / s Mobile Coprocessor for Deep Neural Networks. *2014 IEEE Conference on Computer Vision and Pattern Recognition Workshops*, pages 682–687, 2014.

[27] Aysegul Dundar, Jonghoon Jin, Vinayak Gokhale, Berin Martini, and Eugenio Culurciello. Memory Access Optimized Routing Scheme for Deep Networks on a Mobile Coprocessor. *High Performance Extreme Computing Conference (HPEC), 2014 IEEE*, pages 1–6, 2014.

[28] Samuel Williams, Andrew Waterman, and David Patterson. Roofline: an insightful visual performance model for multicore architectures. *Communications of the ACM*, 52(4):65–76, 2009.

[29] Magnus Halvorsen. Convolutional Neural Network Accelerator, 2015.

[30] Yann LeCun, Corinna Cortes, and Christopher J.C. Burges. MNIST Database, 1998.

[31] Taiga Nomi. Tiny-CNN, 2015.

[32] A Tisan, S Oniga, D MIC, and A Buchman. Digital Implementation of The Sigmoid Function for FPGA Circuits. *ACTA TECHNICA NAPOCENSIS*, 50(2):15–20, 2009.

[33] Jordan L Holt and Jenq-neng Hwang. Finite Precision Error Analysis of Neural Network Hardware Implementations. *IEEE Transactions on Computers*, 42(3):281–290, 1993.

[34] T Chen, Zidong Du, Ninghui Sun, Jia Wang, and Chengyong Wu. Dian-Nao: a small-footprint high-throughput accelerator for ubiquitous machine-learning. *Proceedings of the 19th International Conference on Architectural Support for Programming Languages and Operating Systems*, 2014.

[35] David Bishop. IEEE Purposed Fixed and Floating Point Packages, 2015.

[36] Che W. Lin and Jeen Shing Wang. A digital circuit design of hyperbolic tangent sigmoid function for neural networks. *Proceedings - IEEE International Symposium on Circuits and Systems*, pages 856–859, 2008.

[37] ASUS. ASUS X550JK Specifications, 2015.